



JOINT INSTITUTE FOR NUCLEAR RESEARCH
Dzhelepov laboratory of nuclear problems

FINAL REPORT ON THE START PROGRAMME

Muons track reconstruction in the Top Tracker
detector of the JUNO setup

Supervisor:

Dr. Yury Gornushkin

Student:

Vasilisa Varavina, Russia
Peter the Great St. Petersburg
Polytechnic University

Participation period:

July 06 – August 16,
Summer Session 2025

Dubna, 2025

Abstract

The Jiangmen Underground Neutrino Observatory (JUNO) is scheduled to begin operations in 2025. Prior to full-scale operations, individual detector subsystems — including the Top Tracker muon telescope — are undergoing commissioning tests to ensure reliability and performance. The Top Tracker's primary objective is to reconstruct cosmic muon trajectories, enabling precise vetoing of backgrounds produced by muon interaction with matter, which could otherwise distort measurements from JUNO's central detector. At JINR, a functional prototype of this subsystem has been deployed to validate tracking algorithms and data processing. The prototype enables optimization of data formats, statistical analysis, trigger threshold determination, and calibration procedures under realistic operating conditions. This setup provides essential capabilities for developing and benchmarking track reconstruction algorithms based on precise detector geometry knowledge. Such preparatory work lays critical groundwork for achieving JUNO's ultimate precision in neutrino measurements and contributes to the overall success.

Contents

Abstract	1
Introduction	3
Introduction to the JUNO experiment.....	4
1. Physical fundamentals in the JUNO experiment.....	4
2. Structure and Layout of the JUNO Detector	5
3. Top Tracker design.....	7
4. Data processing	9
5. The TT prototype.....	9
Track construction.....	11
1. Detector and data.....	11
2. Sorting events	11
Conclusion.....	15
Reference.....	16
Acknowledgments.....	17

Introduction

Neutrino — neutral fundamental particles participating only in weak and gravitational interactions. Predicted in 1930 by Wolfgang Pauli to explain energy conservation in beta decay, they were first detected experimentally in 1956 by Clyde Cowan and Frederick Reines. Despite their discovery in 1956, key properties of neutrinos, such as their absolute masses and hierarchy, remain unresolved.

The Jiangmen Underground Neutrino Observatory (JUNO) in China is an international next-generation neutrino experiment having wide programme of studies in neutrino physics from geo-neutrinos to supernova detection. One of the main tasks is to investigate neutrino oscillations, determine the Neutrino Mass Ordering (NMO), and explore potential physics beyond the Standard Model. One of the essential components of JUNO is the Top Tracker system, which plays a crucial role in muon detection and background suppression, enhancing the precision of neutrino measurements.

The objective of this work is the practical study of muon track reconstruction. To achieve this, the following tasks must be completed: studying the theoretical physics behind the JUNO experiment and the detector design (particularly the Top Tracker system), learning to work with ROOT files, and developing analysis code using the ROOT framework.

Introduction to the JUNO experiment

1. Physical fundamentals in the JUNO experiment

Neutrino oscillations are a quantum phenomenon in which a neutrino produced with a specific lepton flavor (such as an electron neutrino) can later be detected as a neutrino of a different type (such as a muon or tau neutrino). This is because the flavour states are a quantum mixture of three mass states with different masses. This is why solar neutrinos that are born as ν_e neutrinos are partially transformed into other types by the time they reach Earth. This behavior implies that neutrinos have non-zero masses, challenging the original Standard Model assumption that they are massless. Neutrinos exist in a quantum superposition of three flavor eigenstates — ν_e (electron neutrino), ν_μ (muon neutrino), and ν_τ (tau neutrino) — which are the states produced in weak interactions (e.g., beta decay, pion decay). However, these flavor states do not correspond to the neutrino's mass eigenstates (ν_1, ν_2, ν_3), which are the true propagating states with definite masses m_1, m_2 and m_3 .

$$\begin{bmatrix} \nu_e \\ \nu_\mu \\ \nu_\tau \end{bmatrix} = \begin{bmatrix} U_{e_1} & U_{e_2} & U_{e_3} \\ U_{\mu_1} & U_{\mu_2} & U_{\mu_3} \\ U_{\tau_1} & U_{\tau_2} & U_{\tau_3} \end{bmatrix} \begin{bmatrix} \nu_1 \\ \nu_2 \\ \nu_3 \end{bmatrix}.$$

Denote $\Delta m_{ij}^2 \equiv m_i^2 - m_j^2$. It is usually defined that the mass of a neutrino is such that $\Delta m_{21}^2 > 0$ and $\Delta m_{21}^2 \ll |\Delta m_{31}^2|$. In such a case, the ranges of mixing parameters are determined by

$$0 \leq \theta_{12}, \theta_{23}, \theta_{13} \leq \frac{\pi}{2},$$
$$0 \leq \delta \leq 2\pi.$$

The sign Δm_{31}^2 defines the neutrino mass hierarchy: $\Delta m_{31}^2 > 0$ (i.e. $m_3 > m_1$) denotes the normal hierarchy (NH) and $\Delta m_{31}^2 < 0$ (i.e. $m_1 > m_3$) denotes the inverted hierarchy (IH).

The standard neutrino oscillation pattern with three flavours is established after observing neutrino oscillation in various neutrino experiments. Neutrino oscillations have been observed in solar, atmospheric, accelerator, and reactor neutrino experiments. To date, two independent neutrino mass-squared differences — $|\Delta m_{31}^2| = |m_3^2 - m_1^2|$ (or $|\Delta m_{32}^2| = |m_3^2 - m_2^2|$) and $\Delta m_{21}^2 = m_2^2 - m_1^2$ — as well as the three mixing angles in the Pontecorvo-Maki-Nakagawa-Sakata (PMNS) parameterization have been measured with a precision of a few percent. Nevertheless, several key questions remain unresolved and will be the focus of future neutrino oscillation experiments: the Neutrino Mass Ordering (NMO), the leptonic CP-violating phase δ in the PMNS matrix, the octant of the mixing angle θ_{23} (i.e., $\theta_{23} < \pi/4$ or $\theta_{23} > \pi/4$) [1].

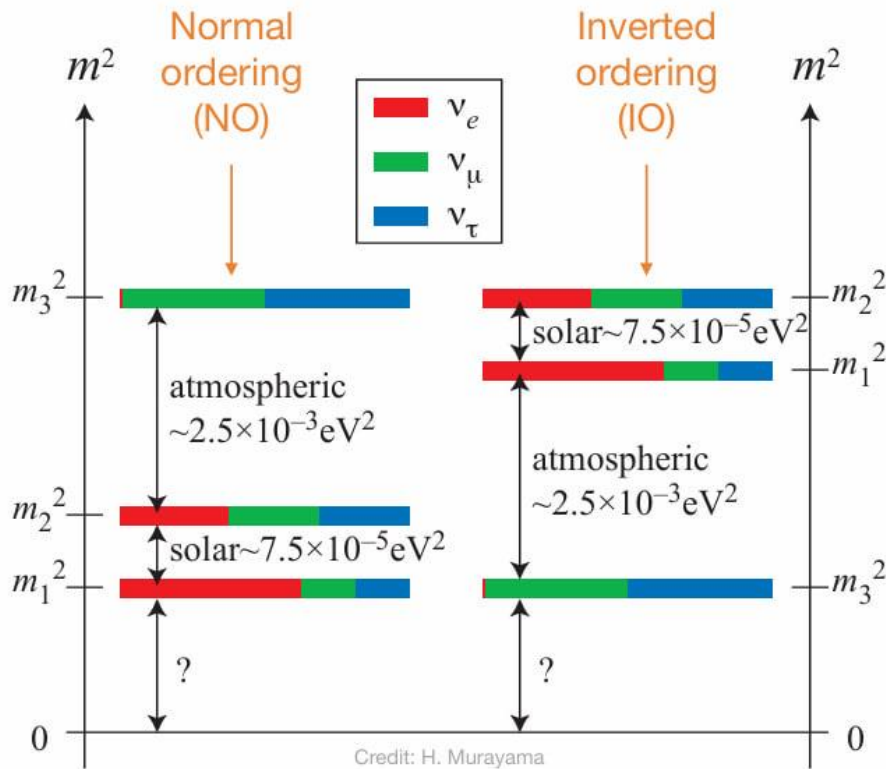
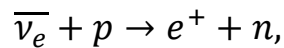


Figure 1. The ordering of the neutrino masses

In the JUNO project inverse beta decay reversal (IBD) is utilized as its primary detection channel



which has established itself as a fundamental tool in experiments with reactor antineutrinos [2].

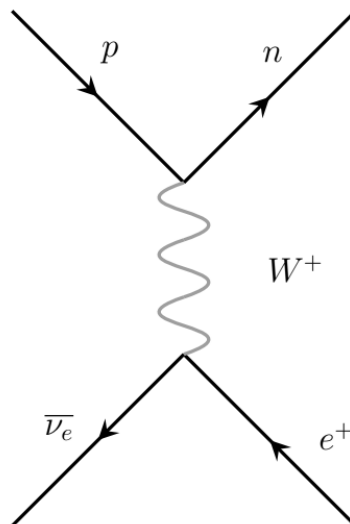


Figure 2. Feynman diagram for Inverse Beta Decay

2. Structure and Layout of the JUNO Detector

The Jiangmen Underground Neutrino Observatory (JUNO) is a state-of-the-art multi-purpose neutrino detector, which construction has been recently completed and which is currently in the commissioning phase. Its primary mission is to resolve the hierarchy of neutrino masses — a fundamental open question in neutrino physics.

The JUNO detector is located approximately 52.5 km from two major nuclear power plants: Yangjiang NPP with 6 reactors (each producing 2.9 GW_{th}), Taishan NPP with 2 reactors (each producing 4.6 GW_{th}), Combined thermal power output: ~26.6 GW_{th}. The chosen baseline of 53 km is optimal for detecting both solar-scale (Δm_{21}^2) and atmospheric-scale (Δm_{31}^2) neutrino oscillation patterns. A smaller auxiliary detector called TAO (Taishan Antineutrino Observatory) is located just 252.5 meters from the Taishan reactor and will precisely measure the antineutrino spectrum to help calibrate JUNO's energy resolution.

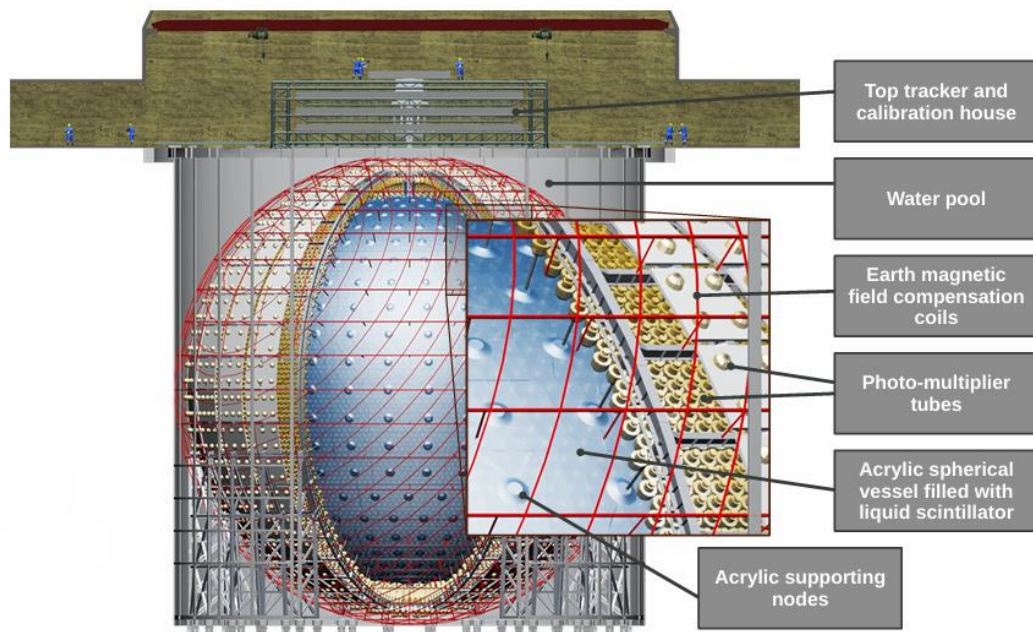


Figure 3. Schematic view of the JUNO detector

The detector is located ~700 meters underground to shield it from cosmic rays and external background. At its core is a 35-meter-diameter acrylic sphere, filled with 20 kilotons of liquid scintillator (LS), which acts as the main neutrino detection medium. This inner volume is surrounded by a water Cherenkov detector, providing active shielding and muon tagging capabilities. Furthermore, key structural components of the JUNO detector include photomultiplier tubes (PMTs) surrounding the inner vessel to capture scintillation light, acrylic supporting nodes that stabilize the large sphere, magnetic compensation coils to reduce Earth's field interference, the Top Tracker detector for precise muon tracking and calibration. Positioned above the central detector, the Top Tracker is an essential subsystem for detecting and reconstructing cosmic muons. The Water Cherenkov Detector (WCD)

and Top Tracker (TT) form a veto system providing both an efficient background reduction towards the environmental radioactivity and the residual cosmic muon flux crossing the detector [3].

3. Top Tracker design

The Top Tracker (TT) of the Jiangmen Underground Neutrino Observatory (JUNO) is a detector originally developed for the OPERA experiment. It consists of 496 plastic scintillator modules from OPERA’s Target Tracker, relocated from the Gran Sasso laboratory (Italy) to China in 2017. The TT serves as a muon tracker, helping to identify and veto cosmic-ray-induced backgrounds that could mimic neutrino signals in JUNO’s central detector.

Each module consists of 64 plastic scintillator strips, each 6.86 meters long and read out on both ends by Wavelength Shifting (WLS) fibers, which channel light to Hamamatsu multianode photomultiplier tubes (MA-PMTs). Four modules are assembled together to construct a tracker plane covering $6.7 \times 6.7 \text{ m}^2$ sensitive surface. Two planes of 4 modules each are placed perpendicularly to form a tracker wall providing 2D track information.

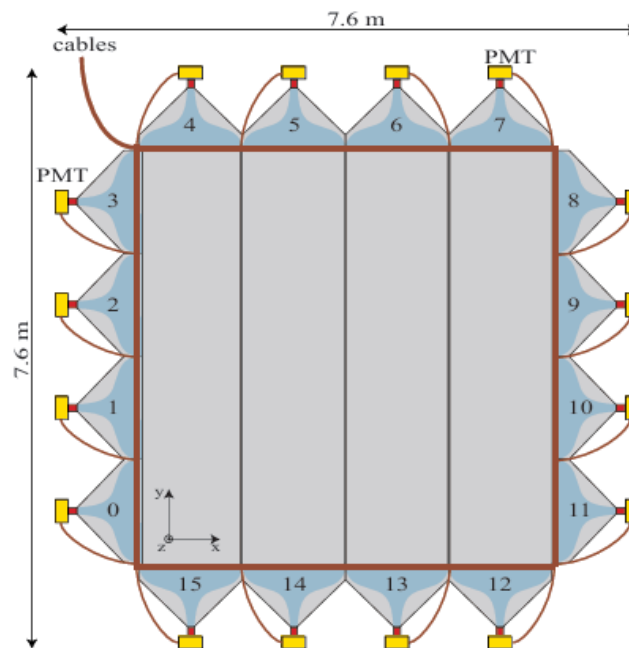


Figure 4. Schematic view of a plastic scintillator strip wall. In addition to the 4 modules clearly visible in the drawing, there are 4 additional modules placed below them in a perpendicular orientation, going for example between the PMTs numbered 0–11

In total, 63 such walls are used, with 60 forming three stacked layers above the detector and three partial walls placed above the calibration chimney to cover that central region. To maintain mechanical stability and optimize muon tracking accuracy, the TT layers are separated vertically by 1.5 meters. The arrangement of

modules ensures substantial coverage (about 60% of the detector’s top area) and provides sufficient lever arm for accurate angular reconstruction. The design enables a spatial resolution on the order of a few centimeters and an angular resolution of approximately 0.2° .

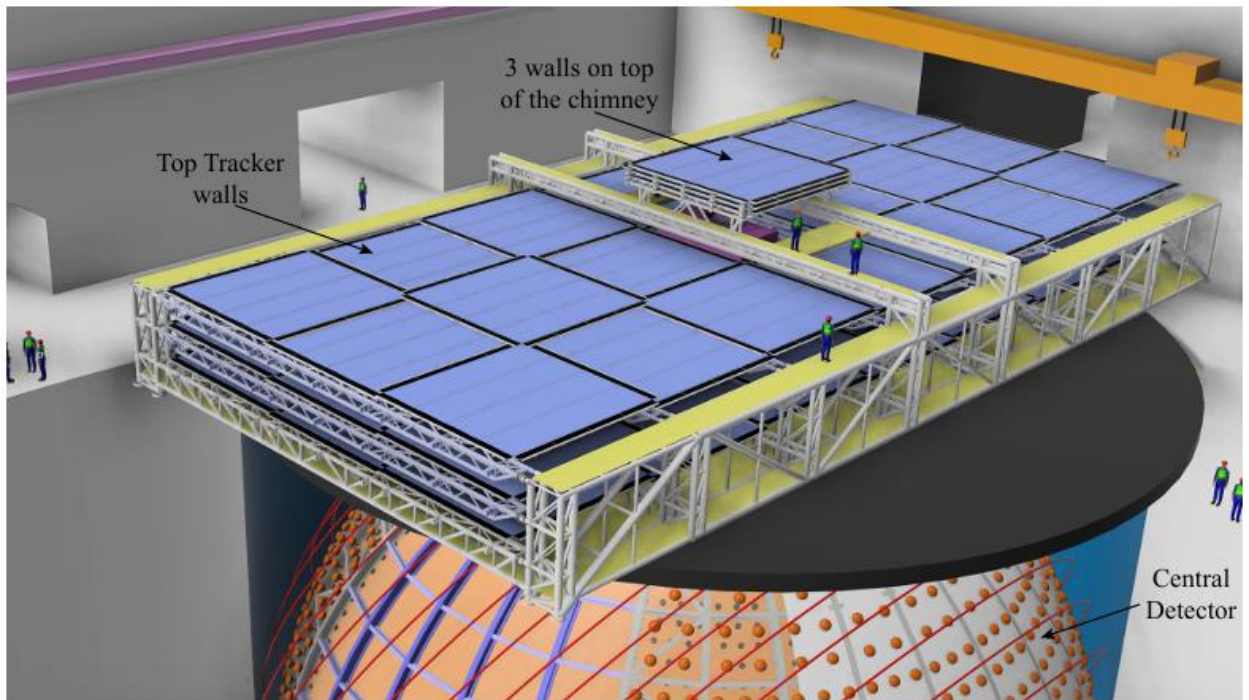


Figure 5. Schematic view of the JUNO Top Tracker on top of the Central Detector

The Top Tracker’s main function is to identify and tag atmospheric muons, which are a source of cosmogenic isotopes like ^9Li and ^8He , as well as fast neutrons. These particles pose a significant background for neutrino detection. JUNO’s underground location (~ 700 meters deep) reduces the muon flux but does not eliminate it. The TT, therefore, forms a key part of the active muon veto system, working together with the water Cherenkov detector.

TT employs a modern readout system based on MAROC3 ASICs, capable of per-channel gain calibration and signal shaping. Each MA-PMT is read out by a Front-End Board (FEB) that interfaces with a ReadOut Board (ROB), and the data are processed further by a Concentrator Board (CB). One CB is placed at the center of each wall and performs a first-level (L1) trigger by identifying time-coincident signals from orthogonal scintillator modules within a 100 ns window. A second-level trigger (L2) is performed by the Global Trigger Board (GTB), which aggregates L1 data from all 63 CBs. It validates events only when coincidences are found across at least three aligned TT walls on different layers, significantly reducing the rate of false events. These multi-level triggers reduce the total event rate from ~ 8 MHz (raw) to just a few kHz, making data acquisition feasible.

The JUNO Top Tracker combines proven OPERA hardware with upgraded electronics to provide precise muon tracking and background rejection. Its three-layer design, fast triggering, and calibration systems ensure high efficiency in

identifying cosmogenic events, supporting JUNO's primary goals in neutrino mass ordering and oscillation studies [4].

4. Data processing

The track reconstruction is divided in three successive steps. In the first step, for each MA-PMT, neighbouring triggered channels are clustered to reduce the impact of the cross-talk in the reconstruction. In the second step, the 3D crossing points of the muon are reconstructed based on information from both perpendicular detection planes of each wall participating in the X–Y coincidence. In the final step, a 3D line is fitted to these 3D points via a χ^2 minimisation. This last step is done independently for every ensemble of more than three 3D points at different vertical positions and fits with a bad χ^2 are rejected.

Before taking specific measurements, calibration must be performed. Top Tracker supports four key operating modes: trigger rate test mode (TRT) for threshold calibration and noise detection, pedestal mode (PED) for determining the base signal level, light injection mode (LED) for calibrating photomultiplier amplification and monitoring their status, and a main data collection mode with zero signal suppression and hybrid readout options. These modes provide complete control over system performance, accurate calibration, and efficient data collection, adapting to the various conditions of the JUNO experiment [4].

5. The TT prototype

To test the electronics under development, a prototype of the TT at JINR was built using the spare modules produced for the OPERA experiment. It is also equipped with the same electronics cards as TT for testing.



Figure 6. Photo of the TT prototype

As shown in Figure 6, the prototype consists of two layers, each of which includes two perpendicular planes. Each plane is assembled from parts of the TT module, cut into two pieces (approximately 1.7 m wide and 3.4 m long). There are left and right ends of the modules, which became the X and Y planes used for alignment, as in the main TT. Unlike full-scale TT modules, which are read from both sides, the prototype is read from only one side. Each of the four module ends is equipped with: MA-PMT (multi-channel photomultiplier), FEB (front-end electronics board), ROB (readout board). All ROB's are connected to a single Concentrator Board (CB) located on the metal frame of the prototype. For testing purposes, it is also possible to read data directly from the ROB, by passing the CB. The prototype made it possible to verify calibration procedures and test interfaces between electronic boards using natural signals (albeit at a slower speed than expected in JUNO due to the lack of high radioactivity in the rock). Working with a prototype helps prepare for data from TT.

Track construction

1. Detector and data

To reconstruct the trajectory of a particle passing through the modules, it is essential to have precise knowledge of the detector's geometry. As already mentioned (Figure 6), the prototype consists of four layers. Module 26 is the topmost layer. Module 518 is positioned 120 mm below module 26 and oriented perpendicularly to it. Module 24 is parallel to module 26, spaced approximately 1 meter apart. Module 516 is placed below module 24, parallel to module 518, and offset by 160 mm relative to module 24. A particle entering from the top sequentially traverses module 24, module 518, module 26, and finally module 516. Each module comprises 64 channels, with a channel pitch of 26 mm, resulting in a total module width of 1,664 mm.

The format of the data received from the detector is defined: a root file containing information about three types of calibration and two trees, TTCycle containing information about time scales and their correspondence, and TTEvent containing information needed to build tracks. In the TTEvent tree, data is divided into events, of which there are about 700,000. Each event has a certain number of hits, and each hit has information about amplitude, time, module, and channel. First, I developed a code that reads the file and outputs events with their relevant information. Below is the data for one sample event:

```
| Event 676932 | cycleEntry = 3599 | nHits = 9 |  
Hit 0: ADC= 44, Module= 26, Time=98714050, Channel=15  
Hit 1: ADC=457, Module= 26, Time=98714050, Channel=31  
Hit 2: ADC=344, Module= 26, Time=98714050, Channel=29  
Hit 3: ADC= 38, Module=516, Time=98714052, Channel= 7  
Hit 4: ADC=231, Module=516, Time=98714052, Channel=16  
Hit 5: ADC=164, Module=516, Time=98714052, Channel=17  
Hit 6: ADC= 68, Module=516, Time=98714052, Channel=25  
Hit 7: ADC=637, Module= 24, Time=98714053, Channel=46  
Hit 8: ADC= 21, Module= 24, Time=98714053, Channel=32
```

Total events in the processed file: 676,934. The available data allows for particle track reconstruction. The coordinate system origin is positioned at the bottom corner of the setup. The detector configuration consists of two perpendicular module pairs - one closely spaced pair and another pair located one meter apart. For reconstruction purposes, the x- and y-modules are considered to share the same z-coordinate corresponding to the midpoint between their physical positions. This configuration provides two measurement planes at fixed z-positions: 80 mm for the near plane and 1085 mm for the far plane. Each plane delivers two-dimensional coordinate data, with one module measuring x-coordinates and the other measuring y-coordinates. The reconstruction assumes particles pass through channel centers, resulting in a 13 mm offset from the origin for the first measurable point (channel 0), with subsequent channels spaced at 26 mm intervals up to a maximum coordinate value of 1651 mm.

2. Sorting events

The initial code was extended to select events containing exactly four hits with one hit in each of the four different modules. This selection criterion ensures the analysis of single-particle events where a particle fully traverses the detection volume defined by all four modules without escaping the boundaries. The four-hit requirement guarantees complete trajectory reconstruction while eliminating partial tracks and multiple-particle events. Each valid event represents a single particle passing through all module layers during one measurement cycle, remaining within the rectangular parallelepiped detection volume.

Thus, for each event meeting the selection criteria, the coordinates of two points, their projections, and zenith angle were obtained. For further analysis, histograms were generated showing the distributions of angles (Figure 7), dx projections (Figure 9), dy projections (Figure 10), and two-dimensional projection distributions (Figure 11).

Output format:

```
| Event 676863 | cycleEntry = 3599 | nHits = 4 |
Hit 0: ADC= 50, Module=518, Time=71467614, Channel=46
Hit 1: ADC=186, Module= 26, Time=71467615, Channel=27
Hit 2: ADC=262, Module=516, Time=71467616, Channel= 5
Hit 3: ADC=292, Module= 24, Time=71467617, Channel=23
Top point = (949.0, 455.0, 1085.0), Bottom point = (611.0, 143.0, 80.0)
dx = -338.0 mm
dy = -312.0 mm
dz = 1005.0 mm
theta = 24.59 deg
```

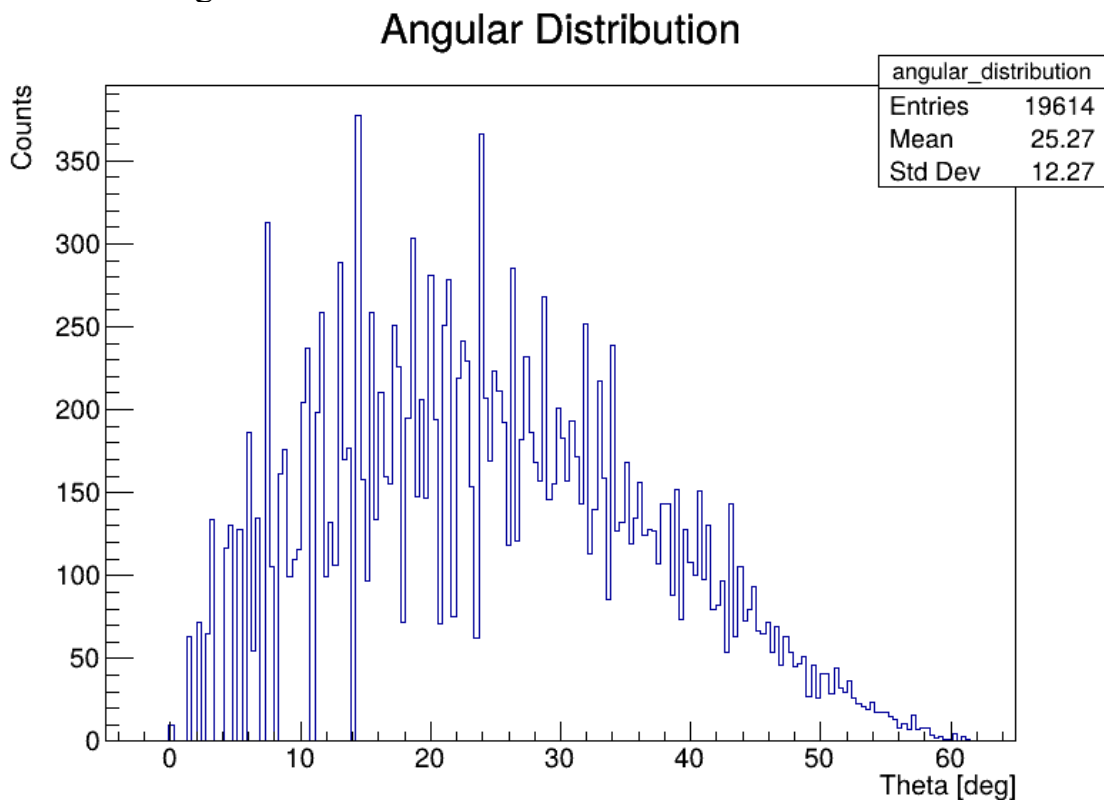


Figure 7. Angular distribution in degrees

X2 - X1 Distribution

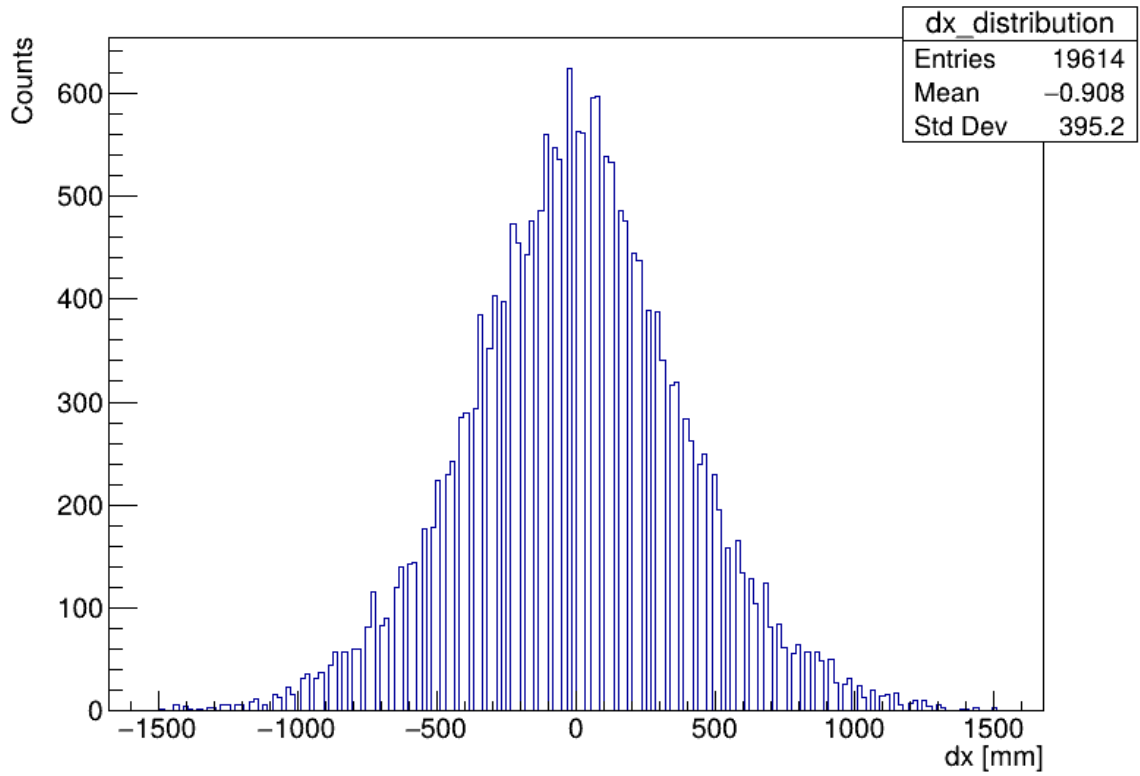


Figure 8. Distribution of projections dx

Y2 - Y1 Distribution

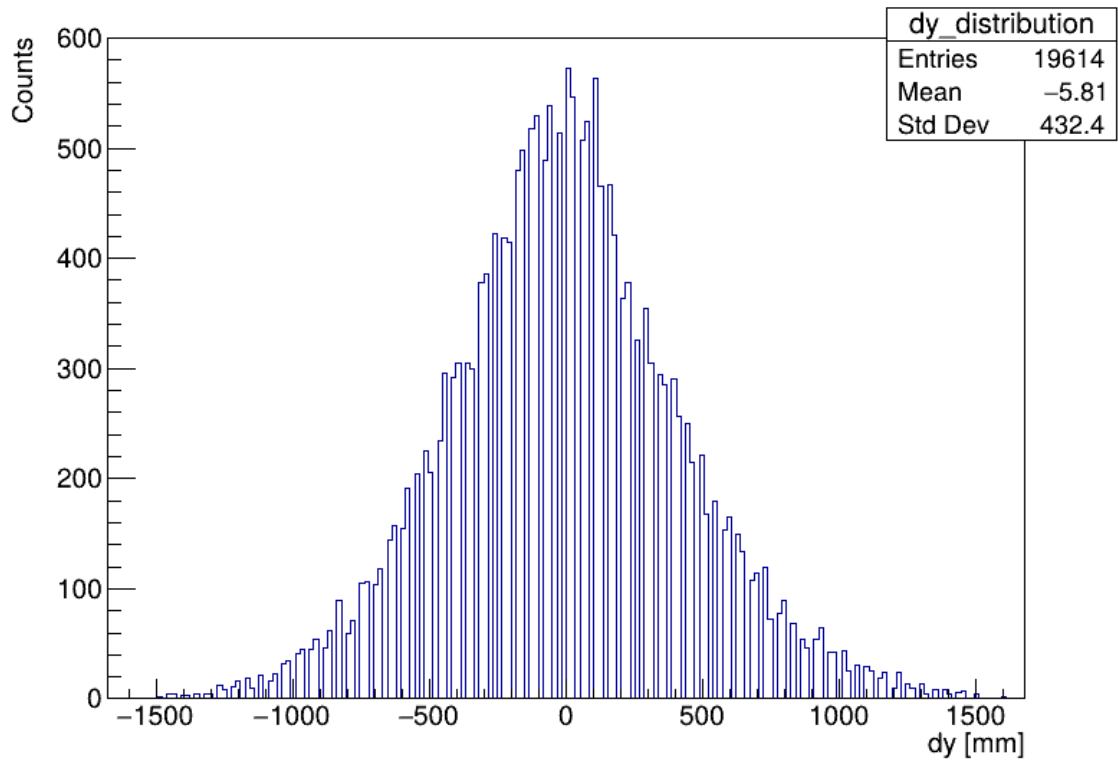


Figure 9. Distribution of projections dy

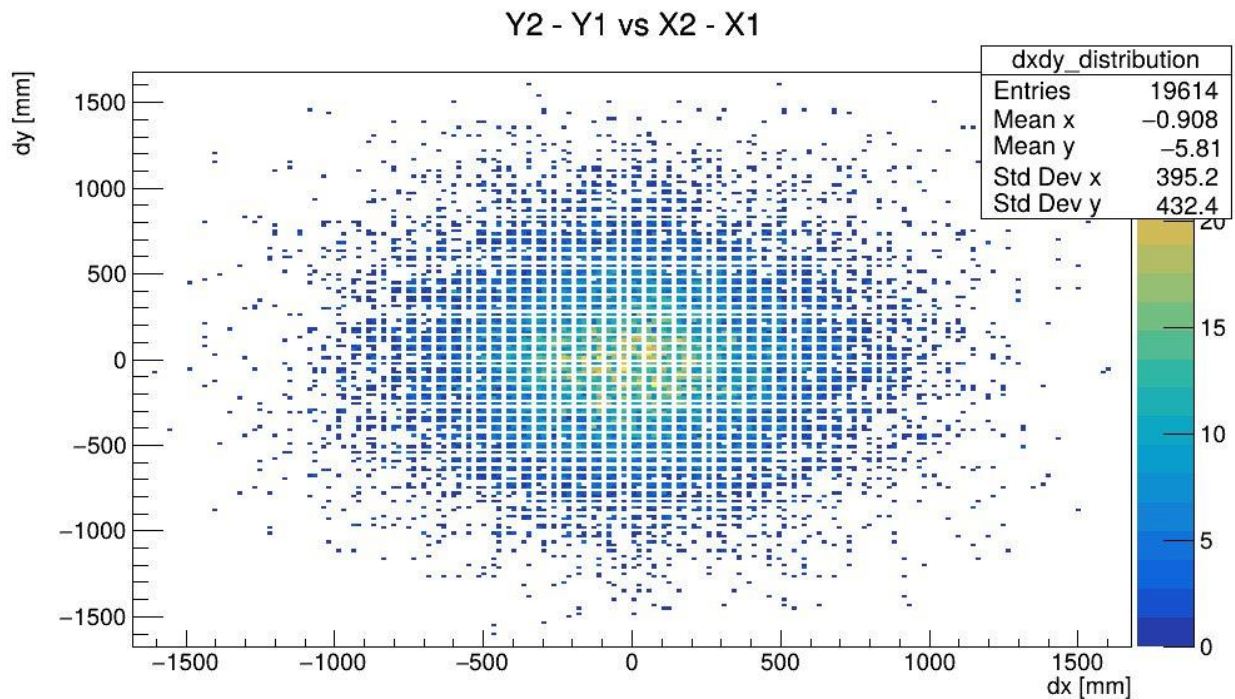


Figure 10. Two-dimensional projection distributions

The projection distributions show that the module planes are divided into points, with 64 points per axis (or $64 \times 64 = 4096$ points per detector plane). The particle trajectories are constrained by the detector geometry, resulting in a maximum incident angle of approximately 60 degrees. As the angle decreases, the number of particles increases, peaking not at zero degrees but between 10-20 degrees. Fewer particles arrived perpendicularly than anticipated.

To estimate the percentage of perpendicular tracks, the first code was modified by adding a condition to match vertically aligned channels in modules measuring the same coordinate. The analysis showed that out of 676,934 events, only 1,453 contained particles with perfectly perpendicular trajectories. The small number of perpendicular tracks can be explained by the assumption that the detector itself is not positioned on a perfectly level surface, which may introduce a slight angular deviation.

Conclusion

The practical training successfully achieved all set objectives, including examination of the theoretical foundations of the JUNO experiment and its detector geometry, acquisition of data processing skills for ROOT file formats, and implementation of analysis algorithms using the ROOT framework. Challenges emerged during the implementation of detector geometry in the code, as the modules were found to be non-identical, requiring special adjustments. This necessitated multiple code revisions as new nuances were continuously discovered. For instance, parallel detectors had opposite channel numbering directions, requiring distinct coordinate transformation algorithms for each type.

The coordinate difference distribution matched expectations: a random variable distribution peaking near zero. However, the angular distribution deviated from predictions - while the maximum was anticipated at zero degrees, the observed peak was shifted. This discrepancy is likely attributable to a slight tilt in the module alignment relative to the horizontal plane, which could have caused the angular offset.

The completed work opens several promising research directions that align with my scientific interests. One such direction is ageing monitoring of scintillator materials. By analyzing particle track data, particularly the angular distributions, we can calculate signal amplitudes normalized per 1 cm of plastic scintillator. Comparing these normalized amplitudes with earlier reference measurements would enable quantitative evaluation of the scintillator's degradation, specifically determining the percentage reduction in registration efficiency over time.

Summing up the results, this summer practical training allowed me to acquire skills in developing an algorithm for muon track reconstruction. This is a valuable skill, as such work is an important part of the veto system in the JUNO experiment.

Reference

- [1] Bellini G. et al. Neutrino oscillations //Advances in High Energy Physics. – 2014. – T. 2014. – №. 1. – C. 191960.
- [2] Vogel P., Beacom J. F. Angular distribution of neutron inverse beta decay, $\nu e + p \rightarrow e^{++} n$ //Physical review D. – 1999. – T. 60. – №. 5. – C. 053003.
- [3] Abusleme A. et al. JUNO physics and detector //arXiv preprint arXiv:2104.02565. – 2021.
- [4] Abusleme A. et al. The JUNO experiment top tracker //Nuclear Instruments and Methods in Physics Research Section A: Accelerators, Spectrometers, Detectors and Associated Equipment. – 2023. – T. 1057. – C. 168680.
- [5] Stock M. R. Status and prospects of the JUNO experiment //arXiv preprint arXiv:2405.07321. – 2024.
- [6] Frühwirth R., Regler M. (ed.). Data analysis techniques for high-energy physics. – Cambridge University Press, 2000. – T. 11.
- [7] F. Reines, C.L. Cowan Detection of the free neutrino, Phys. Rev. Lett., v. 92, p. 830-831, 1953.

Acknowledgments

I would like to express my deepest gratitude to Dr. Yury Gornushkin, my scientific supervisor in the START program, for selecting such an engaging and meaningful project for me, and for assistance through every stage of the work. His patience, attention to detail, and readiness to help me navigate all the nuances and difficulties of the task greatly contributed to my understanding of the subject.

I am equally thankful to the entire START program team and the Joint Institute for Nuclear Research (JINR) for providing me with the unique opportunity to immerse myself, even if only briefly, in the role of a research scientist. This invaluable experience not only allowed me to apply my knowledge in practice but also helped me better understand the real challenges and rewards of scientific work. It will undoubtedly influence my future decisions in both academic and research paths.